An improved multiple model particle filtering approach for manoeuvring target tracking using Airborne GMTI with geographic information

Miao Yu[a], Hyondong Oh[a,*], Wen-Hua Chen[a]

[a]*Department of Aeronautical and Automotive Engineering, Loughborough University, LE11 3TU, UK*

Abstract

This paper proposes a novel ground vehicle tracking method using an airborne ground moving target indicator radar where the surrounding geographic information is considered to determine vehicle's movement type as well as constrain its positions. Multiple state models corresponding to different movement modes are applied to represent the vehicle's behaviour within different terrain conditions. Based on geographic conditions and multiple state models, a constrained variable structure multiple model particle filter algorithm aided by particle swarm optimisation is proposed. Compared with the traditional multiple model particle filtering schemes, the proposed algorithm utilises a particle swarm optimisation technique for the particle filter which generates more effective particles and generated particles are constrained into the feasible geographic region. Numerical simulation results in a realistic environment show that the proposed method achieves better tracking performance compared with current state-of-the-art ones for manoeuvring vehicle tracking.

Keywords: Manoeuvring ground vehicle tracking, geographic information, variable structure multiple models, particle filter, particle swarm optimisation

1. Introduction

Airborne surveillance of moving ground targets is one of important capabilities of manned or unmanned aircraft for both military and civil applications such as search and rescue, border patrol, and infrastructure protection, in which the use of airborne ground moving target indicator (GMTI) radar system is of special interest. As mentioned in [1], the GMTI radar system extracts moving ground target information against a stationary background, providing wide-area, all-weather, day/night, and real time capabilities.

One important preliminary step for the GMTI based airborne surveillance is to continuously estimate vehicle's state information. For instance, in order to analyse if the behaviour of a vehicle in a surveillance region is normal or abnormal, firstly, its position and velocity need to be extracted

---

*Corresponding author
  Email address: `h.oh@lboro.ac.uk` (Hyondong Oh)

[2]. For the continuous estimation of vehicle states, the Kalman or Particle filters based on Bayesian filtering are widely applied [3]. Considering a tracked object could manoeuvre with different movement types, the interactive multiple model (IMM) method was applied for state estimation with multiple state models [4]. To overcome the issues of the non-linear measurement model and the non-Gaussian distribution of the noise component, the interactive multiple models particle filter (IMMPF) was proposed in [5], and the simulation results show the improved performance over the standard IMM method in [4].

Inspired by the fact that the movement of a ground vehicle is not free but constrained by its operational terrains, some terrain information can be combined with certain filtering algorithms. The most widely-used terrain information is the road network, and representative work is shown in [2], [6], [7] and [8]. In [2], the road constraint was treated as a pseudo-measurement and incorporated into the extended Kalman filter (EKF) scheme for state estimation of the target moving on the road. More advanced algorithms were proposed in [6] using the road map information. The target dynamics was modelled in quasi one-dimensional road coordinates and mapped onto ground coordinates using linear road segments, and Gaussian sum approximations and a particle filtering approach were applied and compared. Considering that a moving target is likely to manoeuvre on the road, Cheng *et al.* in [7] applied a multiple model framework to describe the movement of a vehicle, and the unscented particle filtering scheme was proposed for more effective particle generation. In [8], the road width is considered and the road segments are represented in 2-D shapes rather than 1-D line representation. Multiple state models were applied to describe the different vehicle movement and the state model transition probability is set in a state dependent way. An interactive multiple model auxiliary particle filtering (IMMAPF) algorithm was applied which exploits the measurement information when drawing particles.

Arulampalam *et al.* [9] presented a GMTI vehicle tracking problem in which a vehicle could move on or off road and a variable structure multiple model particle filter (VS-MMPF) was applied. For the vehicle's movement on a particular terrain (off-road or a road segment), a corresponding state model was applied to model the vehicle's movement in that terrain. The transition probabilities between state models were set in a state dependent way and the active state models were variable. In [10], instead of using the generic particle filtering approach, the unscented particle filtering scheme was applied in the variable structure multiple model framework to achieve a more accurate state estimation with fewer particles.

In this work, a more realistic scenario is considered in which a vehicle manoeuvres in different terrain conditions with different movement types. Note that a vehicle's movement type and position can be determined by different types of terrain. We exploit both the road topology information and

the off-road terrain information to aid the GMTI tracking compared with aforementioned works which only take the road topology information into account. In order to deal with the multiple movement types of a manoeuvring vehicle, multiple movement modes are considered and related state models are applied for the vehicle's movement description in a particular terrain instead of considering only a single movement mode as in [9] and [10].

The geographic information and multiple modes for movement description are incorporated into a constrained variable structure multiple model particle filter algorithm, aided by the particle swarm optimisation (denoted as C-VSMM-PSO-PF) for an accurate GMTI tracking. The proposed C-VSMM-PSO-PF algorithm applies a particle filtering technique to deal with the non-Gaussian distribution as well as the non-linear GMTI measurements based on a variable structure multiple model (VSMM) scheme. Different from the algorithms in [9] and [10], a particle swarm optimisation technique ([11] and [12]) is introduced to generate more effective particles within a region with comparatively high measurement likelihood values. Finally, particles obtained by performing the PSO which violate the geographic constraints are projected into the feasible geographic regions. The advantages of vehicle tracking using the proposed C-VSMM-PSO-PF algorithm with GIS information and multiple movement modes are validated via numerical simulations.

This paper is organised as follows. Section 2 presents the geographic information-aided state model and the measurement model for describing the GMTI tracking problem. Section 3 proposes the C-VSMM-PSO-PF algorithm. Section 4 shows the advantages of the proposed ground vehicle tracking method from multiple Monte Carlo simulations in a realistic environment. Conclusions are given in Section 5.

2. GMTI tracking models

This section introduces the state and GMTI measurement models for a GMTI tracking problem. Based on these models, certain filtering techniques (such as Kalman or Particle filters [3]) could be developed for state estimation.

2.1. State model description with geographic information

In a realistic environment, different types of terrain conditions exist, and the movement of a vehicle is always constrained by its operational terrains whose information could be collected from geographic information systems (GIS) [13]. When a vehicle moves on the road, it moves along the road segment and its movement is constrained by the road topology. For off-road movement, a vehicle could move in a relatively free way but cannot move on inaccessible regions. Thus, different

3

state models are required to describe the state evolution of a vehicle according to the vehicle's movement characteristics in different terrain conditions.

2.1.1. Off-road state model

As in [14], the state model to describe the off-road movement can be represented as:

$$\mathbf{x}_k^{global} = F\mathbf{x}_{k-1}^{global} + G\mathbf{w}_{global}(m_k) \tag{1}$$

with

$$F = \begin{bmatrix} 1 & 0 & T & 0 \\ 0 & 1 & 0 & T \\ 0 & 0 & 1 & 0 \\ 0 & 0 & 0 & 1 \end{bmatrix}, \quad G = \begin{bmatrix} T^2/2 & 0 \\ 0 & T^2/2 \\ T & 0 \\ 0 & T \end{bmatrix} \tag{2}$$

where $\mathbf{x}_k^{global} = [x_k^{global}, y_k^{global}, \dot{x}_k^{global}, \dot{y}_k^{global}]$ represents the state vector under the real world coordinate system, which includes the real world position ($[x_k^{global}, y_k^{global}]$) and velocity ($[\dot{x}_k^{global}, \dot{y}_k^{global}]$) (here we mainly consider tracking the vehicle's 2-D positions as the height of the vehicle could be derived directly from the GIS as its 2-D positions are known) and T is the interval between consecutive time instances. $\mathbf{w}_{global}(m_k)$ is the uncertain control input of the state model representing the accelerations in different directions. The representation of $\mathbf{w}_{global}(m_k)$ is related to one of the movement mode m_k. To deal with the vehicle manoeuvring with different movement types (such as constant acceleration/velocity or stop), more than one movement mode should be considered and multiple related state models are then be applied to describe the off-road movement.

2.1.2. On-road state model

When a vehicle moves on the road, its movement is determined by the road topology, which mainly follows the road centerline without deviating largely normal to it. In this work, the road network is represented by the connection of straight road segments as in [6] and [7], which could represent the road network in a reasonably accurate way while requiring less computational cost. When a vehicle moves on a particular road segment l_k, its corresponding state model is defined as:

$$\mathbf{x}_k^{l_k} = F'\mathbf{x}_{k-1}^{l_k} + G'\mathbf{w}_{l_k}(m_k) \tag{3}$$

with

$$F' = \begin{bmatrix} 1 & T & 0 \\ 0 & 1 & 0 \\ 0 & 0 & 1 \end{bmatrix}, \quad G' = \begin{bmatrix} T^2/2 & 0 \\ T & 0 \\ 0 & T \end{bmatrix} \tag{4}$$

where $\mathbf{x}_k^{l_k} = [s_k^{l_k}, v_k^{l_k}, n_k^{l_k}]$ represents the state associated with the local coordinate system of road segment l_k. As illustrated in Fig. 1, the origin of the local coordinate system is the starting point a road segment (obtained from the GIS) and two axes are along and normal to the road centerline. Inhere, $s_k^{l_k}$ represents the coordinate in the axis along the centerline, $v_k^{l_k}$ is the corresponding velocity and $n_k^{l_k}$ is the coordinate in the axis normal to the centerline. The control parameter $\mathbf{w}_{l_k}(m_k)$ is related both the road segment and one of the on-road movement modes m_k. Similar to the off-road scenario, multiple movement modes are considered to deal with the vehicle manoeuvring with different movement types on the road.
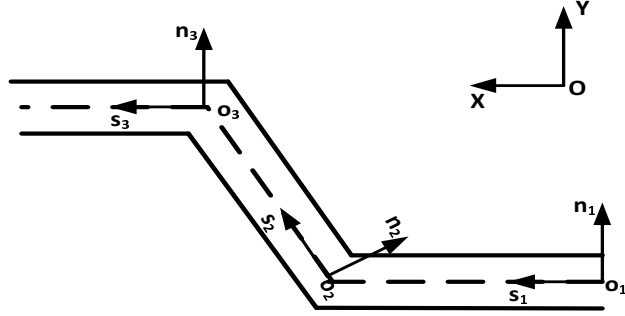

Figure 1: The representations of local road coordinate systems. $o_1 s_1 n_1$, $o_2 s_2 n_2$ and $o_3 s_3 n_3$ represent local road coordinates with respect to different road segments. OXY represents the real world coordinate.

2.1.3. State transition between global/local coordinates

A vehicle could transit from off-road to on-road or vice versa, and its state vector representation needs to be transformed between the global real world coordinate system and local road coordinate system for dynamic modelling in different terrain conditions. For a local state vector $\mathbf{x}_k^{l_t}$, it is converted to its counterpart $\mathbf{x}_t^{global}$ in the real world coordinate system as:

$$x_k^{global} = x_{l_k^{start}} + s_k^{l_k} \cos(\theta_{l_k}) \tag{5}$$

$$y_k^{global} = y_{l_k^{start}} + s_k^{l_k} \sin(\theta_{l_k}) \tag{6}$$

$$\dot{x}_k^{global} = v_k^{l_t} \cos(\theta_{l_k}) \tag{7}$$

$$\dot{y}_k^{global} = v_k^{l_k} \sin(\theta_{l_k}) \tag{8}$$

where $x_{l_k^{start}}$ and $y_{l_k^{start}}$ represent the real world coordinate of the starting point of the current road segment l_k on which a vehicle moves and θ_{l_k} represents the angle of the road segment. $x_{l_k^{start}}$, $y_{l_k^{start}}$ and θ_{l_k} is obtained from GIS.

Conversely, $\mathbf{x}_k^{global}$ is converted back to the local state vector $\mathbf{x}_k^{l_k}$ for a particular road segment

l_k as:

$$s_k^{l_k} = \sqrt{(x_k^{global} - x_{l_k^{start}})\cos(\theta_{l_k})^2 + (y_k^{global} - y_{l_k^{start}})\sin(\theta_{l_k})^2} \tag{9}$$

$$v_k^{l_k} = \dot{x}_k^{global}\cos(\theta_{l_k}) + \dot{y}_k^{global}\sin(\theta_{l_k}) \tag{10}$$

$$n_k^{l_k} = \frac{|y_k^{global} - x_k^{global}\tan(\theta_{l_k}) + x_{l_k^{start}}\tan(\theta_{l_k}) - y_k^{l_k^{start}}|}{\sqrt{1 + \tan(\theta_{l_k})^2}}. \tag{11}$$

2.1.4. Terrain type and movement mode transitions

In a realistic situation, a vehicle moves in different geographic terrains; the movement type of the vehicle also changes due to its manoeuvring. The transition between different terrains is modeled in a state dependent way, which is related to the distance between the vehicle position and the road entry as:

$$p(r_k = \text{on-road}|r_{k-1} = \text{off-road}) = \exp(-c \cdot d) \tag{12}$$

where d is the distance to the entry point of the road network and c is a positive constant value. The transition probability between the on-road and off-road $p(r_k = \text{off-road}|r_{k-1} = \text{on-road})$ has a similar form as in (12), and the only difference is that the distance d is the one to the exit point of the road.

In this work, we apply a simple Markov jump model to reflect the movement mode transition. At time instance $k-1$, we assume that the transition probability to every possible movement modes m_k is equal in order to ensure no bias exists towards a certain movement type.

2.2. GMTI measurement model

A GMTI radar on a UAV platform is assumed to be used, which measures the relative range r and azimuth angle θ of the tracked vehicle at the time instance t given by:

$$\mathbf{y}_k = \begin{bmatrix} r_k \\ \theta_k \end{bmatrix} = \begin{bmatrix} \sqrt{(x_{o,k} - x_k^{global})^2 + (y_{o,k} - y_k^{global})^2 + (z_{o,k} - z_k^{global})^2} \\ \arctan\left(\frac{y_{o,k} - y_k^{global}}{x_{o,k} - x_k^{global}}\right) \end{bmatrix} + \mathbf{n}_k \tag{13}$$

for a recorded measurement $\mathbf{y}_k$, where $(x_k^{global}, y_k^{global}, z_k^{global})$ and $(x_{o,k}, y_{o,k}, z_{o,k})$ represent the real world position of the tracked vehicle and the observer (GMTI tracker) at time instance k, respectively. $\mathbf{n}_k$ represents the radar measurement noise.

There are two problems to be considered for GMTI radar as described below.

2.2.1. Missed detection

A tracked vehicle can-not always be detected, thus its detection will be missed if it does not exist in the line-of-sight (LOS) region of the GMTI radar or the radial velocity (the projected velocity along the line between the GMTI and the tracked vehicle) is below than the minimum detection velocity (MDV) as in [7] (in this case, it is called that the vehicle is within the 'Doppler Blind Zone'). In this work, a similar method to [7] is proposed to model the detection probability considering the effect of the both LOS region and MDV as:

$$
P_D = \begin{cases} 0, & \text{if vehicle is outside LOS region or radial velocity is below MDV} \\ p_d, & otherwise \end{cases} \tag{14}
$$

where p_d is a constant between 0 and 1.

2.2.2. False alarms

In some cases, false alarms will be generated since anything on the ground with significant motion relative to the sensor can trigger a GMTI detection, these false detections are called 'clutter detections'. As in [15], it is usually assumed that the number of the clutter detections follows a Poission distribution and the clutter detections are distributed uniformly across the surveillance region.

To cope with the missed detections and false alarms, a general measurement likelihood function as in [15] is applied to incorporate both the detection probability and clutters distribution, which is represented as:

$$
f(\mathbf{Z}_k|\mathbf{x}_k^{global}) \propto 1 - P_D + P_D \sum_{\mathbf{z}_k \in \mathbf{Z}_k} \frac{g(\mathbf{z}_k|\mathbf{x}_k^{global})}{\gamma c(\mathbf{z}_k)} \tag{15}
$$

where $\mathbf{Z}_k$ is the measurement set at time instance k which contains both true measurement and false alarms (it could also be an empty set with no measurements), γ the expected number of false alarms per GMTI scan, $c(\mathbf{z}_k)$ the uniform spatial distribution of the false alarm and $g(\mathbf{z}_k|\mathbf{x}_k^{global})$ the likelihood function for a measurement element $\mathbf{z}_k \in \mathbf{Z}_k$ conditioned on the global state $\mathbf{x}_k^{global}$, which is determined according to (13).

3. C-VSMM-PSO-PF algorithm

From the state and measurement models mentioned in the last section, different filtering methods could be applied for state estimation. Considering the following two facts: (i) the incorporation of the geographic information into the state equations can significantly distort the distribution of the state vector resulting in non-Gaussian system and (ii) the measurement model of the GMTI

radar is highly non-linear (15), a particle filtering technique is adopted in this work.

A VS-MMPF algorithm was proposed in [9], which applied a particle filtering technique for the state estimation based on a variable structure multiple model (VSMM) framework considering multiple state models to describe on/off road movements and transitions between state models being state dependent. For the generic particle filtering technique, particles are generated only from predictions by the state models in [9], which introduces outlier particles with low measurement likelihood values. To address this issue, the VSMM-UPF (Unscented Particle Filter) framework [10] was proposed in which unscented Kalman filters were applied for new particles generation. Although this method exploits measurement information for new particles generation, as the unscented Kalman filter is performed for every particle, the algorithm becomes computationally expensive.

To further address the above issue, this paper proposes the constrained variable structure multiple model particle filter algorithm, aided by the particle swarm optimisation (C-VSMM-PSO-PF). Firstly, it uses a particle filtering technique based on the VSMM framework considering different movement types (on/off movements), different movement modes and state-dependent model transitions between on/off road. The measurement information is incorporated in new particle generation by applying a particle swarm optimization (PSO) technique to make the outliers converge to a comparatively high measurement likelihood region. Considering the constraints imposed by the geographic information, the resultant particles are projected into the feasible regions determined by the geographic information to meet the constraint conditions. The proposed C-VSMM-PSO-PF algorithm is divided into the following three main steps as follows.

3.1. VSMM prediction

A set of N particles are initialized at $k-1$ as $\{\mathbf{X}_{k-1}^i = [\mathbf{x}_{k-1}^i, l_{k-1}^i, r_{k-1}^i, m_{k-1}^i]\}_{i=1,...,N}$, where each particle $\mathbf{X}_{k-1}^i$ includes the vehicle status (on/off road indicator r_{k-1}^i, movement mode m_{k-1}^i, the particular road segment on which it moves l_{k-1}^i (if r_k^i = off-road, l_{k-1}^i = global)) and the vehicle state vector $\mathbf{x}_{k-1}^i$. New particles for the time instance k are predicted according to the VSMM scheme, which includes:

Status determination: For each particle i, its on/off road indication r_k^i, the road segment l_k^i if it is on-road and the movement mode m_k^i of at time instance k are firstly determined. r_k^i is sampled according to the probability as in Eq. (12), m_k^i is chosen from the possible movement modes with an equal probability and l_k^i is determined by the following criteria:

$$l_k^i = \begin{cases} \text{global}, & r_k^i = \text{off-road} \\ l_{start}, & r_{k-1}^i = \text{off-road} \ \text{ and } \ r_k^i = \text{on-road} \\ l_{k-1}^i & r_k^i = \text{on-road} \end{cases} \tag{16}$$

where l_{start} represents the road segment which is the entry to a road network.

State prediction: According to $\{l_k^i, r_k^i, m_k^i\}_{i=1,...,N}$ and vehicle states $\{\mathbf{x}_{k-1}^i\}_{i=1,...,N}$ in the particle set, new N vehicle states at the time instance k are predicted according to Eq. (1) (for r_k^i = off-road) or Eq. (2) (for r_k^i = on-road) and denoted as $\{\mathbf{x}_k^{predict,i,l_k^i}\}_{i=1,...,N}$. Note, if $r_k^i \neq r_{k-1}^i$, the corresponding state vector $\mathbf{x}_{k-1}^i$ needs to be transformed before state prediction.

Status/state adjustment: For a r_k^i = on-road and the along-centerline axis coordinate of $\mathbf{x}_k^{predict,i,l_k^i}$ (denoted as s) is larger than the length of the road segment l_k^i (denoted as L) or smaller than zero, a new road segment which connects to the end or start point of the road segment l_k^i is chosen to replace the original l_k^i. The coordinate in the along-centerline axis of $\mathbf{x}_k^{predict,i,l_k^i}$ is adjusted to $s_k^{predict,i,l_k^i} - L$ or $-s_k^{predict,i,l_k^i}$. After the VSMM prediction step, a new set of particles $\{\mathbf{X}_k^{predict,i} = [\mathbf{x}_k^{predict,i,l_k^i}, l_k^i, r_k^i, m_k^i]\}_{i=1,...,N}$ is obtained.

3.2. Particle swarm optimisation

Note that vehicle states $\{\mathbf{x}_k^{predict,i,l_k^i}\}_{i=1,...,N}$ included in the predicted N particles may be 'outliers' which fall into a very low measurement likelihood region. To mitigate this issue, the particle swarm optimisation (PSO) [11], a population based stochastic optimisation technique, is applied to make the predicted vehicle states converge into a comparatively high measurement likelihood region (as illustrated in Fig. 2) by maximising the likelihood function in Eq. (15).

The predicted states $\{\mathbf{x}_k^{predict,i,l_k^i}\}_{i=1,...,N}$ are taken as an initial population set for the PSO algorithm. For the consensus of the vehicle states' coordinates, all the vehicle states are transformed into the real word coordinate system as $\{\mathbf{x}_k^{predict,i,global}\}_{i=1,...,N}$ using Eqs. (5)$\sim$(6). Then, for each $\mathbf{x}_k^{predict,i,global}$, a fitness value $f(\mathbf{Z}_k|\mathbf{x}_k^{predict,i,global})$ is estimated. After estimating the fitness values for the initial population set, the individual best $\mathbf{p}_0^i$ for every individual i and global best $\mathbf{g}_0$ are estimated as described in [11]. Based on the individual best and global best, every individual i moves with a velocity of $\mathbf{v}_0^i$, which relates to the difference between the individual i and the individual/global best, and a new population set is obtained. The velocity $\mathbf{v}_0^i$ is . For the new population set, the same procedure repeats as the initial one to obtain individuals with higher fitness values. The population set update continues until certain conditions are met (e.g. the maximum iteration number is reached or the function values for the majority of points are larger than a pre-specified threshold, as illustrated in more details in the numerical simulations section).

Technical details of the PSO are explained in Algorithm 1. r_1 and r_2 in Algorithm 1 are random numbers with Gaussian distribution $N(0,1)$, and ρ is a zero-mean Gaussian perturbation noise added to avoid particles being trapped in local optima. The obtained population set after performing the PSO, $\{\mathbf{X}_k^{optimised,i} = [\mathbf{x}_k^{optimised,i}, l_k^i, r_k^i, m_k^i]\}_{i=1,...,N}$ is obtained to replace the original set $\{\mathbf{x}_k^{predict,i,l_k^i}\}_{i=1,...,N}$ for a new set of particles.

Algorithm 1 Particle Swarm Optimisation to obtain more effective particles

Input: $\{\mathbf{x}_0^i\}_{i=1,...,N} = \{\mathbf{x}_k^{predict,i,global}\}_{i=1,...,N}$ is chosen as the initial population set.

1: Set $j = 0$, $\mathbf{p}_0^i = \mathbf{x}_0^i$ for $i = 1, ..., N$, $\mathbf{g}_0 = \arg\max_{\mathbf{p}_0^i} f(\mathbf{Z}_k|\mathbf{p}_0^i)$ for $i = 1, ..., N$

2: **while** Termination condition is not met **do**

3:     $j = j + 1$

4:     **for** $i = 1$ to N **do**

5:         $\mathbf{v}_j^i = |r_1|(\mathbf{p}_{j-1}^i - \mathbf{x}_{j-1}^i) + |r_2|(\mathbf{g}_{j-1} - \mathbf{x}_{j-1}^i) + \rho$

6:         $\mathbf{x}_j^i = \mathbf{x}_{j-1}^i + \mathbf{v}_j^i$

7:         $\mathbf{p}_j^i = \begin{cases} \mathbf{x}_j^i & if \ \ f(\mathbf{Z}_k|\mathbf{x}_j^i) > f(\mathbf{Z}_k|\mathbf{p}_{j-1}^i), \\ \mathbf{p}_{j-1}^i & otherwise. \end{cases}$

8:     **end for**

9:     $\mathbf{g}_j = \arg\max_{\mathbf{p}_j^i} f(\mathbf{Z}_k|\mathbf{p}_j^i)$ for $i = 1, ..., N$

10: **end while**

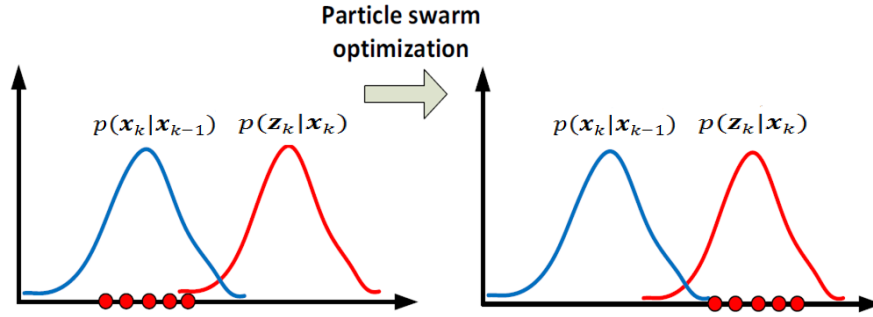**Output:** $\{\mathbf{x}_k^{optimised}\}_{i=1,...,N} = \mathbf{g}_j$

Figure 2: The illustration of particle swarm optimisation, which makes particles generated from the state transition probability converge into a region with comparatively high measurement likelihood value

3.3. Particles projection and state estimation

Finally, the geographic information which constrains the vehicle's movement is considered. The geographic constraint regions are sometimes non-linear so, in this work a projection based method as in [16] which is a simple but efficient technique to deal with different types of constraints, is applied to exploit the geographic constraint information. For the particle $\mathbf{X}_k^{optimised,i} = [\mathbf{x}_k^{optimised,i}, l_k^i, r_k^i, m_k^i]$ obtained from the PSO optimisation, if the vehicle position is not within the feasible region (outside the road boundary if r_k^i = on-road or inside the off-road infeasible region if r_k^i = off-road), then it is projected to the nearest point on the feasible region boundary. In this way, it is guaranteed that obtained particles meet the geographic constraints. The particles after projection are denoted as $\{\mathbf{X}_k^{projection,i} = [\mathbf{x}_k^{projection,i}, l_k^i, r_k^i, m_k^i]\}_{i=1,...,N}$.

The probability of a vehicle being on/off road $p(r_k)$, the movement mode probability $p(m_k)$ and the state estimation $\hat{\mathbf{x}}_k^{m,r}$ corresponding to an off/on road movement type ($r_k = r$) with a particular

movement mode ($m_k = m$) are obtained as:

$$p(r_k = r) = \sum_i w_i, \quad for \quad i \in \{j|r_k^j = r\} \tag{17}$$

$$p(m_k = m) = \sum_i w_i, \quad for \quad i \in \{j|m_k^j = m\} \tag{18}$$

$$\hat{\mathbf{x}}_k^{m,r} = \frac{\sum_i w_i \mathbf{x}_k^{projection,i}}{p(m_k = m, r_k = r)}, \quad for \quad i \in \{j|r_k^j = r, m_k^j = m\}, \tag{19}$$

where $w_i \propto f(\mathbf{Z}_k|\mathbf{x}_k^{projection,i})$ as in Eq. (15).

The on/off road type (denoted as $r_{vehicle}$) and the movement mode (denoted as $m_{vehicle}$) of the vehicle are determined by achieving the largest $p(r_k)$ and $p(m_k)$. The final state estimation of the vehicle is then $\hat{\mathbf{x}}_k^{m_{vehicle}, r_{vehicle}}$. After the state estimation, for every particle i whose $r_k^i =$ on-road, the vehicle state vector $\mathbf{x}_k^{projection,i}$ is converted back to the local coordinate for the VSMM prediction at the next time instance using Eq. (9). The outline of the proposed C-VSMM-PSO-PF algorithm is presented in Algorithm 2.

Algorithm 2 The outline of the C-VSMM-PSO-PF algorithm

Input: N particles are initialised at $k-1$ as $\{\mathbf{X}_{k-1}^i = [\mathbf{x}_{k-1}^{i,l_{k-1}^i}, l_{k-1}^i, r_{k-1}^i, m_{k-1}^i]\}_{i=1,...,N}$

●*VSMM prediction:*
   Obtaining the on/off road movement type r_k^i, road segment l_k^i movement mode m_k^i and predicted state $\mathbf{x}_k^{i,l_k^i}$ according to corresponding transition probabilities for every particle. Every predicted state $\mathbf{x}_k^{predict,i,l_k^i}$ is converted to the global one $\mathbf{x}_k^{predict,i,global}$ for PSO.

●*PSO:*
   Taking the predicted vehicle states $\{[\mathbf{x}_k^{predict,i,global}\}_{i=1,...,N}$ as an initial population, a new set of vehicle states $\{\mathbf{x}_k^{optimised,i}\}_{i=1,...,N}$ is obtained from PSO using Algorithm 1

●*Particle projection:*
For the obtained vehicle state particles $\mathbf{x}_k^{optimised,i}$ whose position is outside the feasible region, we project the vehicle position to the nearest point on the feasible region's boundary to obtain a new set of vehicle state particles $\{\mathbf{x}_k^{projection,i}\}_{i=1,...,N}$.

●*State estimation:*
The final particle set at time instance k is obtained as $\{\mathbf{X}_k^i = [\mathbf{x}_k^{projection,i}, l_k^i, r_k^i, m_k^i]\}_{i=1,...,N}$. The on/off road probability, movement mode probability and vehicle state are obtained using Eqs. (17)~(19). After the state estimation, the corresponding $\mathbf{x}_k^{projection,i}$ is converted back to the local road segment state for $r_k^i =$ on-road. The VSMM prediction for the next time instance is then performed and the above procedure repeats.

---

4. Numerical Simulations

The advantages of the proposed C-VSMM-PSO-PF algorithm are evaluated by numerical simulation study. We simulate a scenario that a UAV platform with the GMTI radar tracks a highly manoeuvring vehicle in a realistic environment (a region of Lindifferon, St. Andrews in the United

Kingdom). The simulated vehicle trajectory is plotted as the blue line in Fig. 3. The satellite image in Fig. 3 is geo-referenced with the British National Grid (BNG) coordinate system to represent the real world position (the origin of this coordinate system is located at $49°N, 2°W$). x and y axes represent the distance to the origin along the East and North direction, respectively.

The on/off road transition, movement modes transitions and velocity amplitude variations corresponding to the simulated vehicle movement are plotted in Fig. 4. The time interval between two consecutive time instances is one second and the vehicle's movement lasts for 87 seconds. The vehicle moves in a highly manoeuvring way, which approximates a realistic scenario wherein a vehicle moves in different terrain conditions and does not always follow a particular manoeuvring type. The state models corresponding to on/off road movements have forms of Eqs. (1) and (2) as

Figure 3: The trajectories of the simulated UAV (red stars) and vehicle (blue line) movements. The satellite image is taken from Google Earth and geo-referenced.
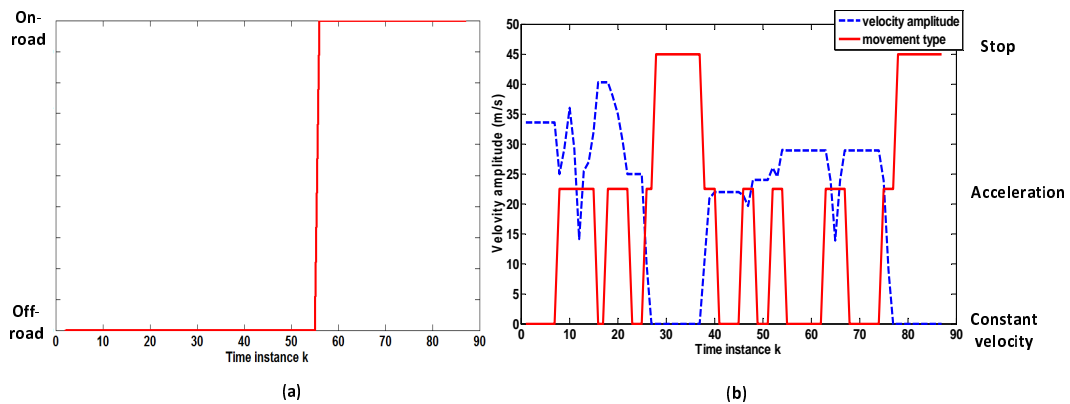

Figure 4: The transitions of the vehicle's movement types. (a) on/off road movement transitions (b) velocity and movement mode variations

described in Section 2, and three types of movement modes (CV, CA and Stop) are considered in this work. The control parameter $\mathbf{w}_{global}(m_k)$ for the off-road movement with different movement

modes is presented in Eq. (20).

$$\mathbf{w}_{global}(m_k) \sim N(\mathbf{w}|\mathbf{0}, \begin{bmatrix} (0.1)^2 & 0 \\ 0 & (0.1)^2 \end{bmatrix}) \quad for \quad (m_k = CV)$$

$$\mathbf{w}_{global}(m_k) \sim N(\mathbf{w}|\mathbf{0}, \begin{bmatrix} (15)^2 & 0 \\ 0 & (15)^2 \end{bmatrix}) \quad for \quad (m_k = CA) \qquad (20)$$

$$\mathbf{w}_{global}(m_k) = \begin{bmatrix} -\dot{x}_k^{global} \\ -\dot{y}_k^{global} \end{bmatrix} \quad for \quad (m_k = Stop)$$

where $\mathbf{w}_{global}(m_k)$ is assumed to follow Gaussian distribution for CV and CA movement mode. The standard deviations of the components of $\mathbf{w}_{global}(m_k)$ are set to be small for CV to reflect the movement with a constant velocity and those for the CA mode are set large to deal with the vehicle manoeuvring. For the Stop model, the control parameter is set to a deterministic value to guarantee the velocity to become zero.

Similarly, the control parameter $\mathbf{w}_{onroad}(m_k)$ of the on-road state model corresponding to different on-road vehicle in Eq. (21) is set as:

$$\mathbf{w}_{l_k}(m_k) \sim N(\mathbf{w}|\mathbf{0}, \begin{bmatrix} (0.1)^2 & 0 \\ 0 & \sigma_n^2(l_k) \end{bmatrix}) \quad for \quad (m_k = CV)$$

$$\mathbf{w}_{l_k}(m_k) \sim N(\mathbf{w}|\mathbf{0}, \begin{bmatrix} (15)^2 & 0 \\ 0 & \sigma_n^2(l_k) \end{bmatrix}) \quad for \quad (m_k = CA) \qquad (21)$$

$$\mathbf{w}_{l_k}(m_k) = \begin{bmatrix} -v_k^{l_k} \\ 0 \end{bmatrix} \quad for \quad (m_k = Stop)$$

where the standard deviation for the first component of $\mathbf{w}_{l_k}(m_k)$ (representing the acceleration along the road centerline) is set in the same way as in the off-road movement scenario. The second component of $\mathbf{w}_{l_k}(m_k)$ represents the change of the normal distance for consecutive time instances whose standard deviation $\sigma_n(l_k)$ is related to the width of the particular road segment l_k (obtained from the GIS) for CV and CA movement modes.

A GMTI radar sensor is assumed to be mounted on a moving Unmanned Aerial Vehicle (UAV) platform for monitoring. We simulate the UAV loitering at an altitude of 200 m where the circle radius is 100 m and angular speed is $\pi/20 \; rad/s$ (the UAV trajectory in the 2-D overlook plane is marked as red stars in Fig. 3). Measurements of the GMTI radar are simulated according to Eq. (13) with a Gaussian noise being added to the relative range and angle between the vehicle and the UAV platform. The Gaussian noise is assumed to have zero mean and the standard deviations

13

for r and θ are: $\sigma_r = 5$ m and $\sigma_\theta = 0.05$ rad, respectively. It is assumed that the vehicle is always within the line-of-sight of the sensor. If the radial velocity between the vehicle and the GMTI radar is smaller than the threshold (set to 1 m/s in this work), no vehicle measurements are obtained; otherwise, corresponding measurements are generated with a detection probability of p_d which is set to be 0.9. The expected number of false alarms (γ in Eq. (15)) is set to 2 and false alarms are assumed to be spatially equally distributed across the surveillance area in Fig. 3.

The geographic information for the surveillance area is obtained from the GIS. In the GIS, different types of terrains such as the off-road wood/building regions or the road network and their corresponding geographic information (area of a terrain region, real world positions, region boundary, etc.) are available from corresponding geographic datasets. Figure 5 represents the visualisation of different types of terrain regions on a geo-referenced image in the surveillance area, obtained from the Ordnance Survey OpenData [17]. Based on this simulation scenario, evaluations
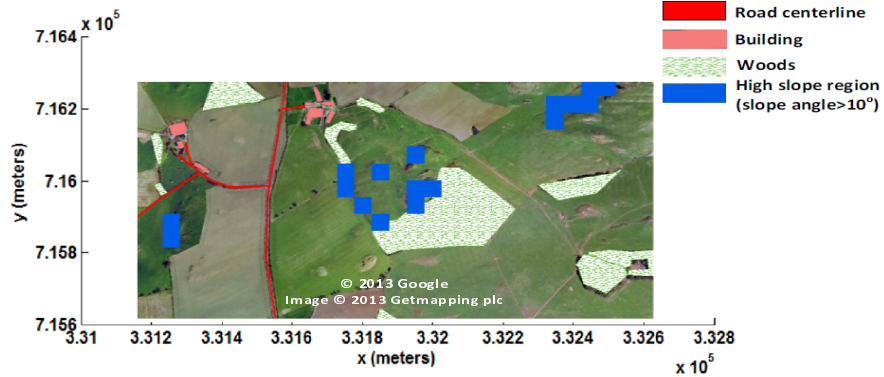

Figure 5: The presentation of different types of terrains on a georeferenced image. Terrain information is obtained from GIS.

are performed as described below.

4.1. PSO termination conditions

In our work, the termination conditions of the PSO in our proposed C-VSMM-PSO-PF algorithm are set as:

(i). Values of measurement likelihood function (15) for a certain amount of particles (50% of whole particle number set in the algorithm implementation) are no smaller than a particular threshold (set by 0.1), or

(ii). The maximum allowed iteration number (denoted as i_{max}) is reached. Condition (i) guarantees that a certain percentage of particles are not 'outliers', but in a comparatively high measurement likelihood region with proper levels of likelihood function values and condition (ii) determines the maximum allowed execution time of PSO algorithm.

For a comprehensive analysis, we evaluate the influences of different numbers of i_{max} on the performance of our algorithm. The comparison results are shown as in Table 1, from which we can see that as i_{max} increases we can obtain smaller mean and standard deviation of RMSE errors. However, as i_{max} reaches to a certain value, the additional increasing of i_{max} will not gain too much improvements. For example, as the i_{max} increases from 5 to 10, there is a reduction of 3.46 (corresponding to 24% reduction) of the RMSEs mean. And as the i_{max} increases from 10 to 20, the reduction of the RMSEs mean is 0.12 (corresponding to only a 1% reduction). In our work, $i_{max} = 10$ is chosen for the implementation of the C-VSMM-PSO-PF algorithm and used for the evaluations in the following sections.

Table 1: The performance comparison for different estimation algorithms.

i_{max} value	Mean (meters)	Std (meters)	Computation time (seconds)
0	19.14	2.90	3.18
5	14.53	2.05	3.66
10	11.07	1.15	4.30
20	10.95	1.07	4.49

4.2. Geographic information evaluation

Next we analyze the effect of incorporating the geographic information in terms of the tracking performance. The proposed C-VSMM-PSO-PF algorithm is compared with its counterpart without incorporating any GIS information. If no geographical information is used, the state model in Eq. (1) is always applied to describe the vehicle movement (no road information is applied) and there are no geographic constraints. Otherwise, different models as mentioned in Section 2 are applied to describe the on/off road movements and the infeasible region (including the woods, building and high slope regions as marked in Fig. 5 and regions outside the road boundary when the vehicle moves on road) are exploited to constrain the particles as in Section 3.

50 trials of Monte-Carlo simulations are performed. For each Monte-Carlo simulation, one tracking result against the ground truth trajectory is obtained for each approach (with/without geographic information) and 50 different tracking results for each approach are obtained. At every time instance, the 50 times averaged root mean square errors (RMSEs) between tracking results and ground truth trajectory are plotted in Fig. 6 (a) and averaged on/off road probabilities are plotted in Fig. 6 (b). From the results, we can see that estimated on/off road probabilities coincide with the groundtruth ones and smaller RMSEs are obtained during the majority of time instances by the aid of different types of geographic information. We also calculate the RMSEs between the whole

15

ground truth trajectory and the tracked results for each approach. The mean and covariance of 50 RMSEs are summarised in Table 2, from which we can see that by incorporating the geographic information, improved tracking performance is obtained with more than 40% improvement of the mean tracking error.
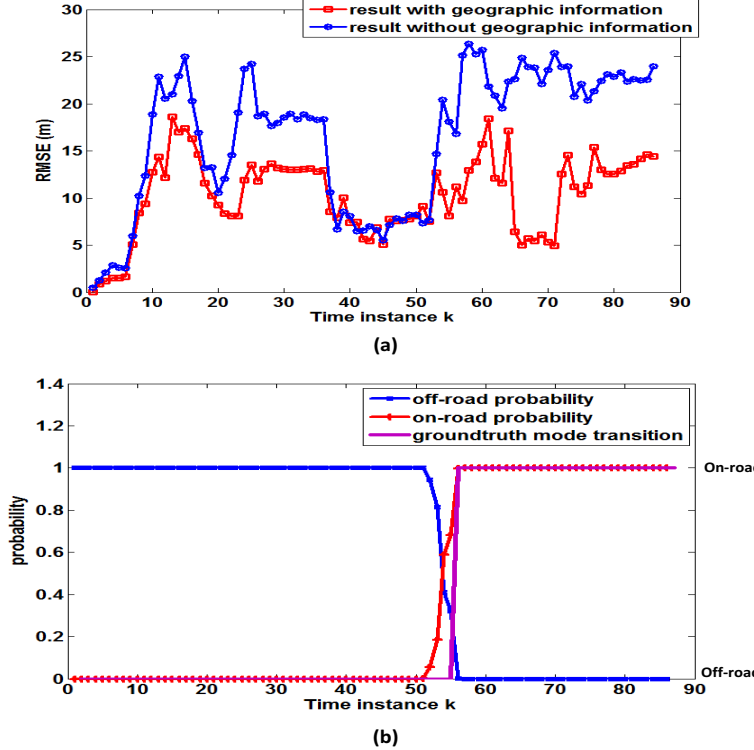

Figure 6: The 50 times averaged RMSEs and on/off road probabilities for every time instance. (a). the comparison of 50 times averaged RMSEs at every time instances for approaches with/without geographic information (b). the 50 times averaged on/off road probabilities.

Table 2: The estimation performance comparison with and without the geographic information.

	Mean (meters)	Std (meters)
No geographic information	19.42	2.43
Geographic information	11.07	1.15

4.3. Evaluation of incorporating multiple movement modes

We analyze the advantage of considering different movement modes ($m_t = AC$, $m_t = CV$ and $m_t = Stop$) and applying corresponding state models (as in Eqs. (20)) and (21)) for describing both the on/off road movements. We compare our multiple movement mode scheme with the one in [9] and [10] which only considers a single movement mode for vehicle movement description. For

the single movement mode scheme, the mode $m_t = AC$ is chosen for comparison considering the corresponding state model's ability to catch up with the vehicle manoeuvring highly.

For a quantitative analysis, 50 Monte-Carlo simulations are performed for vehicle tracking.The mean and standard deviation of RMSEs between the tracking results and ground truth trajectory for single and the multiple movement mode scheme are presented in Table 3, from which we can see that a significant improvement (more than 50% over the mean of RMSEs) is obtained by considering multiple movement modes. Besides, the movement type of vehicle is also estimated by the proposed multiple model scheme. The probabilities of the 'stop' and 'non-stop' movement modes are estimated and presented in Fig. 7. It is observed that modes with larger estimated probabilities at different time instances are consistent with the ground truth ones as in Fig. 4 (b).
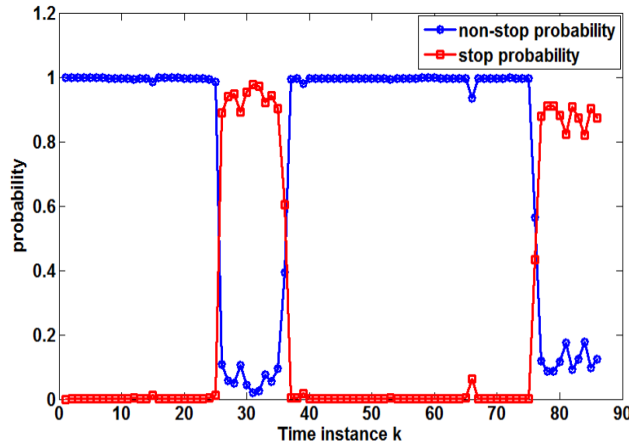

Figure 7: The 50 times averaged stop/non-stop probabilities for every time instance.

Table 3: Performance comparison with different state model schemes for movement description.

	Mean (meters)	Std (meters)
Single movement model	25.82	5.73
Multiple movement models	11.07	1.15

4.4. Algorithm evaluation

Finally, we compare the proposed method with other particle filtering based algorithms, which include: VSMM-PF [9], VSMM-UPF [10] and the extension of the differential evolution-Markov chain particle filtering [18] for variable structure multiple models framework (VSMM-DEMC-PF). For a fair comparison, all the methods incorporate the GIS information by projecting invalid particles into the feasible region and the algorithms then become constrained versions of them (termed

as C-VSMM-PF, C-VSMM-UPF, and C-VSMM-DEMC-PF). 50 trial Monte-Carlo simulations are
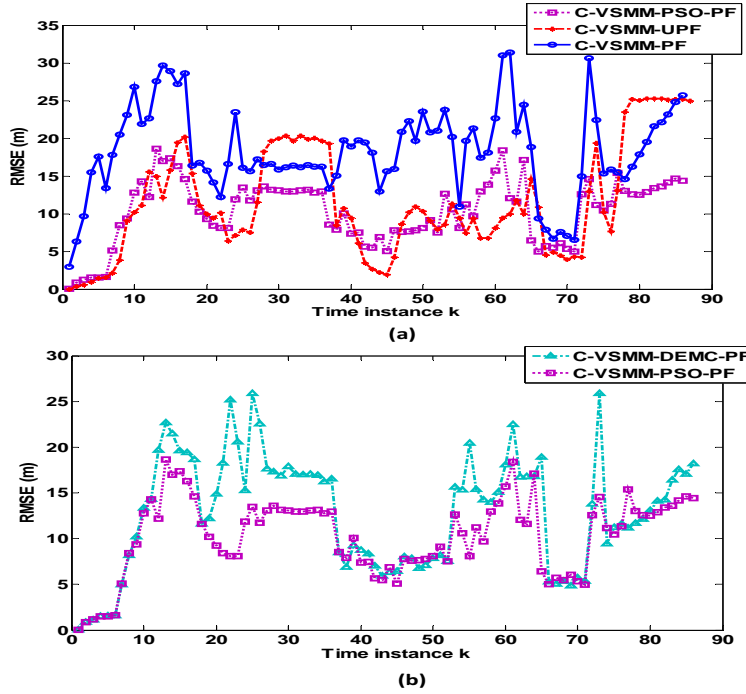

Figure 8: The comparison of RMSEs at different time instances between different algorithms.

performed and the corresponding RMSEs at different time instances for different algorithms are plotted in Fig. 8. The mean and variance of RMSEs, between the whole ground truth trajectory and 50 tracking results by different algorithms are represented in Table III. For every algorithm, the averaged computation time for each trial is also presented for efficiency analysis.

From the results, it can be observed that the C-VSMM-PF algorithm exhibits the worst tracking accuracy. The RMSEs are larger than its counterparts during the majority of time as shown in Fig. 8 (a), and it has largest mean and standard deviation of the RMSEs as shown in Table III. This is because no measurement information is exploited for particles generation in the C-VSMM-PF algorithm. The generated particles are likely to be less effective outliers and thus resulting in a poor state estimation result.

The C-VSMM-UPF and C-VSMM-DEMC-PF make use of measurement information for more efficient particle generation. However, compared with those two, the proposed method (C-VSMM-PSO-PF) achieves even better performance as shown in Table III. It also shows much higher computational efficiency than C-VSMM-UPF. Here, the reduction in the computational cost is due to the avoidance of the time-consuming unscented Kalman filtering process for every particle. It is worthwhile noting that the proposed method achieves much better performance than C-VSMM-UPF when the vehicle stops (time instances 26-36 and 77-87 seconds) from Fig. 8 (a). This is

18

because when the vehicle stops, no measurements related to the vehicle will be received according to the characteristic of the GMTI radar. For the C-VSMM-UPF algorithm, only the mode transition probability and the state model are applied to obtain the mode and vehicle state. However, the PSO technique integrated in the proposed method makes the particles converge to the high measurement likelihood region, which corresponds to the Doppler blind zone with small velocities.

Table 4: The performance comparison for different estimation algorithms.

Algorithms	Mean (meters)	Std (meters)	Computation time (seconds)
C-VSMM-PF	19.14	2.90	3.18
C-VSMM-DEMC-PF	14.09	2.34	4.19
C-VSMM-UPF	13.94	1.72	18.14
C-VSMM-PSO-PF	11.07	1.15	4.30

Lastly, similar to the proposed method, the C-VSMM-DEMC-PF generates more effective particles by maximising the measurement likelihood by applying the DEMC algorithm. Compared with the DEMC algorithm, the PSO algorithm makes use of the individual best *and* global best information to generate new populations (as explained in Algorithm 1), rather than generating new populations randomly as for the DEMC. In this way, more effective particles with high measurement likelihood values are generated by the proposed C-VSMM-PSO-PF scheme. As shown in Fig. 8 (b), the RMSEs for the proposed algorithm is smaller than those for the C-VSMM-DEMC-PF during the majority of the time.

5. Conclusions

This work has proposed a novel method for manoeuvring ground vehicle tracking using a GMTI radar. It is considered that in a realistic scenario a tracked vehicle's movement is constrained by the geographic conditions and it may manoeuvre in different ways. More comprehensive on/off road geographic information is exploited to constrain the movement of the tracked vehicle according to the environment, and multiple movement modes are applied to describe the vehicle manoeuvring on/off road. Based on the geographic information and multiple movement modes, the C-VSMM-PSO-PF algorithm is proposed which incorporates the PSO scheme into the VSMM-based particle filtering scheme to obtain more effective particles by exploiting the measurement information in a more efficient way. Comprehensive numerical simulations on a realistic scenario are performed to demonstrate the advantages of the proposed method.

References

[1] R. Sullivan, Radar Foundations for Imaging and Advanced Concepts, SciTech Publishing Inc., 2004.

[2] H. Oh, S. Kim, A. Tsourdos, Road-map assisted standoff tracking of moving ground vehicle using nonlinear model predictive control, IEEE Transactions on Aerospace and Electronic Systems 51 (2) (2015) 975–986.

[3] B. Ristic, S. Arulampalam, N. Gordon, Beyond the Kalman Filter: the Particle Filters for tracking applications, Norwood, MA: Artech House, 2004.

[4] E. Mazor, A. Averbuch, Y. Shalom, J. Dayan, Interacting multiple model methods in target tracking: a survey, IEEE Transactions on Aerospace and Electronic Systems 34 (1) (1998) 103–123.

[5] Y. Boers, J. Driessen, Interacting multiple model particle filter, IEE Procceding-Radar Sonar and Navigation 150 (5) (2003) 344–349.

[6] M. Ulmke, W. Koch, Road-map assisted ground moving target tracking, IEEE Transactions on Aerospace and Electronic Systems 42 (4) (2006) 1264 –1274.

[7] Y. Cheng, T. Singh, Efficient particle filtering for road-constrained target tracking, IEEE Transactions on Aerospace and Electronic Systems 43 (4) (2007) 1454 –1469.

[8] M. Yu, C. Liu, W. Chen, J. Chambers, A Bayesian framework with auxiliary particle filter for GMTI based ground vehicle tracking aided by domain knowledge, in: Proc. of SPIE, Signal Processing, Sensor/Information Fusion, and Target Recognition XXIII, Baltimore, MD, USA, 2014.

[9] M. Arulampalam, N. Gorden, M. Orton, B. Ristic, A variable structure multiple model particle filter for GMTI tracking, in: Proceedings of the Fifth International Conference on Information Fusion, Annapolis, MD, USA, 2002.

[10] O. Payne, N. Gordon, A. Marrs, An unsented particle filter for GMTI tracking, in: 2004 IEEE Aerospace Conference, Big Sky, Montana, USA, 2004.

[11] X. Zhang, W. Hu, S. Maybank, A smarter particle filter, in: 9th Asian Conference on Computer Vision, Xi'an, Chian, 2009.

[12] M. Wachowiak, R. Smolikova, Y. Zheng, J. Zurada, A. Elmaghraby, An approach to multi-modal biomedical image registration utilizing particle swarm optimization., IEEE Transactions on Evolutionary Computation 8 (3) (2004) 289–301.

[13] S. Bhattacharjee, P. Mitra, S. Ghosh, Spatial interpolation to predict missing attributes in GIS using semantic kriging, IEEE Transactions on Geoscience and Remote Sensing 52 (8) (2014) 4771–4780.

[14] T. Kirubarajan, Y. Bar-Shalom, Tracking evasive move-stop-move targets with a GMTI radar using a VS-IMM estimator, IEEE Transactions on Aerospace and Electronic Systems 39 (3) (2003) 1098–1103.

[15] B. Vo, B. Vo, A. Cantoni, Bayesian filtering with random finite set observations, IEEE Transactions on Signal Processing 56 (4) (2008) 1313–1326.

[16] X. Shao, B. Huang, J. Lee, Constrained bayesian state estimation: A comparative study and a new particle filter based approach, Journal of Process Control 20 (2) (2010) 143–157.

[17] https://www.ordnancesurvey.co.uk/business-and-government/products/opendata-products.html, accessed in September 2015.

[18] M. Du, X. Nan, L. Guan, Monocular human motion tracking by using DE-MC particle filter, IEEE Transactions on Image Processing 22 (10) (2013) 3852–3865.